

Application-Specific Energy Management Systems for Electric Vehicles Based on Charge and Discharge

Mr. Mailappan¹(P.G Scholar)·Mrs.A.Sridevi² M .E,

,Dept of Electrical and Electronics ,Dept of Electronic and Communication ,Dept of Electrical and Electronic
AdithyaInstitute of Technology,
Kurumbapalayam
Annauniversity-Chennai
mailappanvijay@gmail.com

Abstract— This paper presents solar based electric vehicle (EV) charging circuit. Incremental Conductance MPPT Algorithm is used to extract maximum power from the solar PV at STC conditions. A battery of rating 100AH is charged with the solar PV panel using a boost converter which generates output voltage of 400V. Then the voltage is stepped down for buck operation according to 220V battery requirement. The SOC characteristic is observed to be fully charged within short period. The passive parameters (filter components on the input and output) of the system are derived and appropriately used in the work. Also in the absence of solar PV energy, electric vehicle is charged from the grid. A PR (proportional plus resonant) controller is used with a corner frequency of 10rad/sec. A 400 V dc output voltage is obtained through a H-bridge rectifier and applied to a DC-DC bidirectional converter. It is observed that the battery SOC is accomplished within a small period. During charging and discharging modes the battery voltage and current is presented. It is clear that the grid voltage and current are in phase during charging. During discharging they are said to be out of phase indicating the reverse power flow. IGBT switches are considered to be operating at 10 kHz. On-board electric vehicle chargers can be utilized at homes and parking places. The work reflects the usage of EV connected to solar exhibits less dependency on the grid with clean (zero emission) and smooth movement of the vehicle.

Index Terms— Battery, Electric vehicle, maximum power point, proportional resonant controller, State of Charge.

I. INTRODUCTION

Solar Energy can be utilized for electric vehicle (EV) battery charging applications in urban areas. Hence the burden on the grid gets reduced when EV's are directly integrated to the solar charging stations [1]. Therefore, in this work, a solar power based EV charging is proposed.

Fig. 1 shows the electric vehicle charging with solar PV, the electric vehicle charging with grid as well as with the solar PV [2]-[6]. In the day time the electric power generated by the solar PV is utilized to charge EV. In absence of the solar PV power, the electric vehicle is charged with the power grid. Electric vehicle charging circuit with solar PV

configuration consisting of two stages is referred in [7]-[8]. First stage acts as a converter/inverter and the second stage consists of a DC-DC converter which acts as step-up converter during discharging and as a buck converter during charging. The battery is used to store electrical energy in the form of chemical energy in charging and energy is supplied to grid during discharging.

In EV the battery plays an important role, SOC (state of charge) of the battery is maintained within the limits for long life. There are different types of batteries which are used in the EV, they are Nickel-cadmium, Lead-acid and Lithium-ion batteries. Lithium-ion batteries are preferred for EV due to high specific energy, good discharging capabilities and long working life [9]. Section II deals with the EV circuit configuration and passive components design, section III deals with EV Charging with solar PV. Section IV deals with EV with proportional plus resonant controller (PR) in charging, section V deals with the EV Support to Grid.

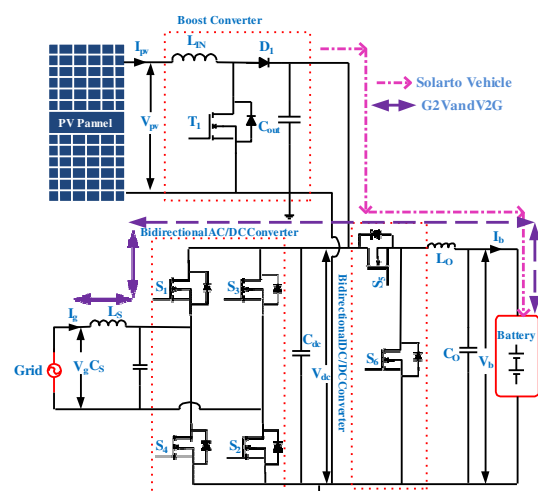


Figure 1. Electric Vehicle with Solar Charging Configuration

II. VCIRCUITCONFIGURATIONANDDESIGN

An effective design of the passive filters used in the circuit is very much necessary for the best operation of the EV. The design of passive components are presented here for the EV considered in the work [10].

(i) DC bus capacitor (C_{dc}):

In single phase converters output DC voltage consists of second order harmonics and hence a large value of dc Capacitor on the dc side is required. The dc capacitor is an energy storage device between the input and output. The capacitor value will be selected based on its energy storage. The input power is given by (1) assuming the input power factor to be unity,

$$P_{in} = v_{in} \times i_{in} = \frac{VI}{2} - \frac{VI}{2} \cos 2\omega t \quad (1)$$

Input inductor power is given by (2)

$$P_L = \frac{\partial \left(\frac{1}{2} L (I \sin \omega t)^2 \right)}{\partial t} = \omega L I^2 \sin \omega t \cos \omega t \quad (2)$$

The energy flows from input inductor to the H-bridge converter and charges the output dc capacitor. Neglecting the device power losses, power in the output capacitor is equal to the difference between the input power and inductor power. The power flow through the capacitor (is obtained using (3))

$$P_C = P_{in} - P_L = \left(\frac{VI}{2} - \frac{VI}{2} \cos 2\omega t \right) - \omega L I^2 \sin \omega t \cos \omega t \quad (3)$$

In equation (3) DC component is supplied to DC output and second order components will charge and discharge the capacitor which causes ripple in output DC voltage. For a half cycle, the instantaneous power is calculated by simplifying and taking the integration, (4) represents the ripple energy

$$E_C = \int_0^{2\pi} \left[\frac{VI}{4} + \frac{\omega LI}{4} \sin 2\omega t \right] dt = \frac{\sqrt{VI + \omega LI}}{4} / \omega \quad (4)$$

From the ripple energy in the capacitor, one can derive the relation between DC capacitor, DC voltage and input inductor as (5)

$$C_{dc} = \frac{\sqrt{\frac{V^2 I^2}{4} + \frac{\omega^2 L^2 I^4}{4}}}{2 \times V_{dc} \times \Delta V_{dc} \times \omega} \quad (5)$$

Using (5), C_{dc} is obtained to be 2mF.

(ii) Input side filter (L_s and C_s):

The filter inductor is designed based on the ripple current flowing through the inductor (L_s).

$$L_s = \frac{V_{dc} \times \left(\frac{V \sin \omega t}{V_{dc}} \times \left| 1 - \frac{V \sin \omega t}{V_{dc}} \right| \right)}{2 \Delta I f_{sw}} \quad (6)$$

V_{dc} is the DC voltage with ripple and instantaneous value of input AC voltage is given by $V \sin \omega t$, f_{sw} is the switching frequency and ripple current ΔI is taken as 10% of the input current. The harmonics of the output voltage is damped by using the input LC filter capacitor and is given by (7)

$$C_s = \frac{1}{2\pi f_{sw}} \times \frac{1}{L_s} \quad (7)$$

The capacitor filter C_s and inductor L_s are obtained as 20μF and 0.75 mH.

(iii) Output filter (L_o and C_o):

The output filter inductor L_o and capacitor C_o are calculated using (8) and (9) respectively.

$$L_o = \frac{1}{2f_{sw}} \quad (8)$$

$$C_o = \frac{(1-D)}{8L_o \left(\frac{\Delta V_o}{V_o} \right)^2 f_{sw}^2} \quad (9)$$

The output side capacitor required is very large to maintain the output voltage constant. duty ratio is D , the internal resistance is r , f_{sw} switching frequency of the buck/boost converters, V_o is

The output voltage, ΔV_o is ripple voltage which is 5% of the Output voltage. L_o and C_o is obtained to be 41μH and 600 μF. A 120V rms 60Hz single phase system is considered in this work.

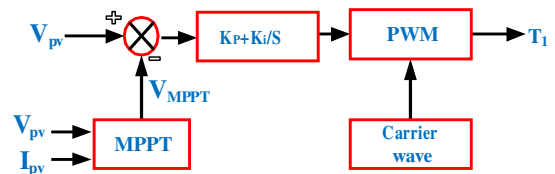


Figure 2. PV Boost Converter Control Circuit

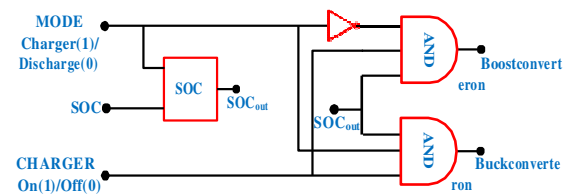


Figure 3(a). Upper level control

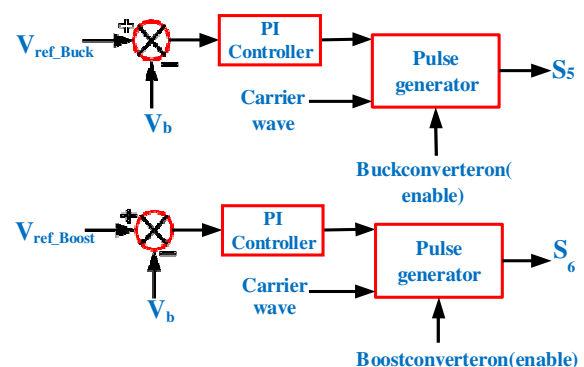


Figure 3(b). Lower level control for DC-DC Converter

Fig. 2 shows the solar PV boost converter control circuit, PV array voltage and the MPPT voltage is compared and voltage error is generated. Error voltage generated flows through proportional plus integral controller (PI) and PI controller output is compared with 10 kHz triangular carrier wave, according to it switching pulses are generated for PV boost converter. The upper level and lower level controllers for the bidirectional DC-DC converter is shown in Fig.3 (a) and 3(b). In upper level control according to the battery SOC between 5% to 100% and mode of operation i.e. charging or discharging mode, SOC_{out} is derived. Then SOC_{out} and Charger ON/OFF are given to the logic circuits to produce signal for enable the buck or boost converter. Accordingly switching pulses are regenerated using Fig.3(b) to the switches of the Buck/Boost converter. Similarly for lower level control the switching pulses are generated based on the voltage error and buck converter on signal.

III. ELECTRIC VEHICLE CHARGING WITH PV

The Electric vehicle battery is charging with the solar PV energy in the day time. The circuit configuration is as shown in Fig. 1. The PV panel voltage is boosted up to 400 volts by using a step-up converter. PV boost converter voltage is step down according to the battery voltage requirements by using DC-DC converter. Here battery capacity of 100AH, 230 V (20 kWh) is considered. An Onboard charging circuit at Home or parking places can be realized. Table I shows the Boost converter design parameters and Fig. 4 shows the PV panel with input labels and table II shows array parameters used for simulation.

Simulation results of the electric vehicle charging with the solar PV are discussed. Switching pulses obtained for the solar PV boost converter is shown in Fig. 5. The switching pulses obtained for the buck converter during charging is shown in Fig. 6. Fig. 7 shows the characteristics of the solar PV at STC conditions (25°C, 1000 Lumens). A 220 V open circuit voltage and 2.5 A short circuit current is obtained with PV panel parameters shown in Table II.

TABLE I PARAMETERS OF PV BOOST CONVERTER

Parameters	Value
Boost converter input voltage	200V
Output Voltage	400V
Input inductor, L_{IN}	1.3mH
Output capacitor, C_{out}	2500 μ F
Duty ratio	0.5
Switching frequency	10kHz

Fig. 8 shows the solar PV voltage and MPPT voltage tracking, the PV array takes 0.122s time to track the MPPT reference voltage (V_{mppt}) and 0.5% steady state error. Fig. 9 shows the boost converter output voltage 400V. Battery Fig. 10 shows the battery voltage and the current. Fig. 11 shows the battery state of charge during the EV charging. It is observed that the electric vehicle is charged 100% with solar PV within a short period (10s).

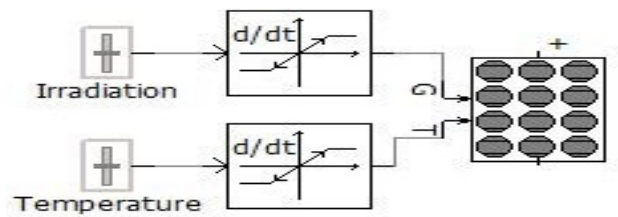


Figure 4. PV panel with input labels (Source: PSCAD software simulator)

TABLE II PARAMETERS OF PV ARRAY

PV Array	Value
Modules connected in series in one array	7
Module strings in parallel in one array	10
Cells connected in series in one module	36
Cell strings in parallel in one module	1
Irradiation taken as reference	1000L
Cell reference temperature	25°C

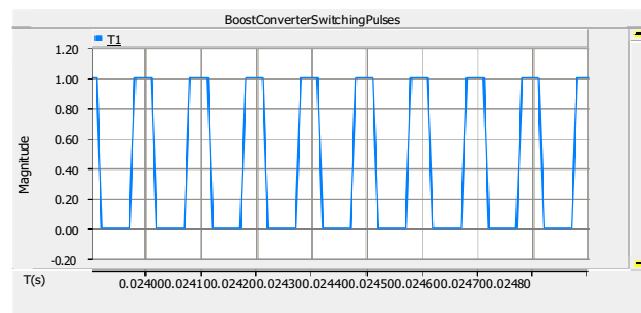


Figure 5. PV Boost Converter Switching pulses (T_i)

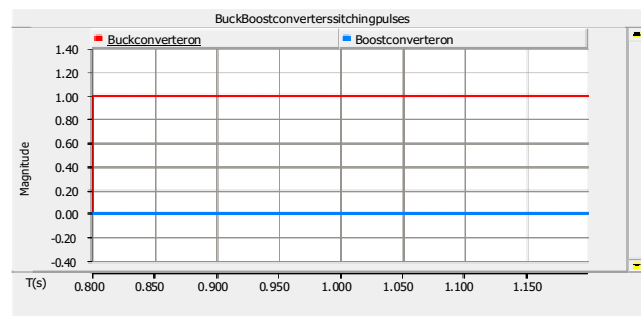


Figure 6. Buck Converter Switching Pulses (ON) and Boost Converter (OFF)

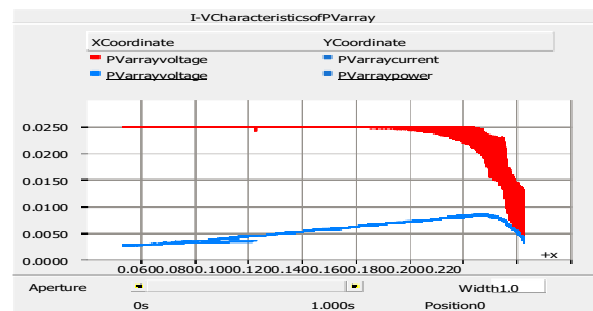


Figure 7. Characteristics of solar PV

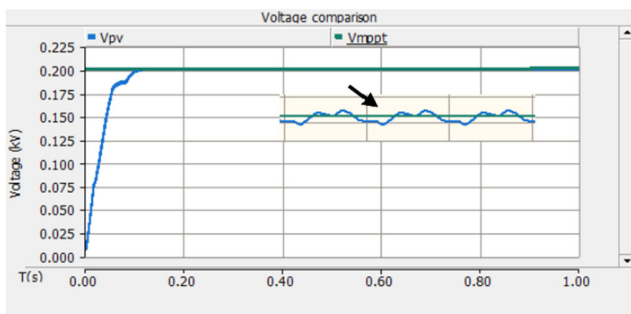


Figure 8. Solar PV Array and MPPT Voltages Tracking

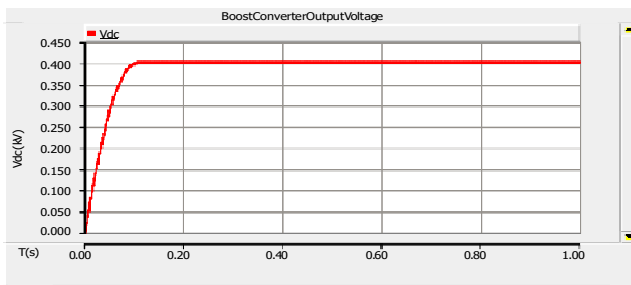


Figure 9. Boost Converter Output DC Voltage

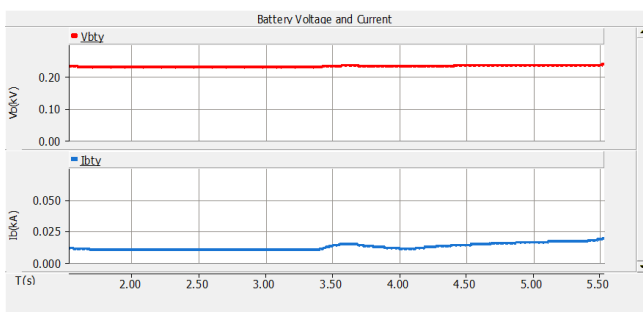


Figure 10. Battery charging Voltage and Current

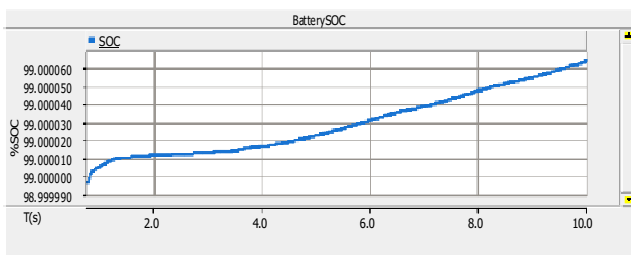


Figure 11. Battery State of Charge during charging

IV. ELECTRIC VEHICLE CHARGING FROM GRID

In this mode of operation the electric vehicle is charged from the grid. This mode operates in the absence of the solar power. The electric vehicle charging from grid circuit configuration is shown in Fig. 1 and system parameters used for simulation is shown in Table III. The switching pulses for the single phase H-bridge bidirectional converter is generated by using proportional pulse resonant (PR) controller. The control block diagram of the PR controller is shown in Fig. 12. PR introduces at the fundamental frequency an infinite gain and has a ability to follow the sine current waveform [11] with reduced steady state error. To avoid stability problems at infinite gain, an approximate high gain low pass filter which is

basically a second order transfer function is used as a non-ideal PR controller in this work.

The PR controller $G_{PR}(s)$ is given by (10)

$$G_{PR}(s) = k_p + k_i \frac{2\omega_c s^2}{s^2 + 2\omega_s s + \omega_o^2} \quad (10)$$

System dynamic response is determined by k_p , phase shift between the output and the reference input is adjusted by using k_i , cut off frequency $\omega_c \ll \omega_o$, resonant frequency ω_o is kept at 377 rad/s in this work. Here $k_i = k/\omega_c$ assumed to simplify the controller. It is taken here as unity so that the effect of ω_c can more easily be understood [12]-[13].

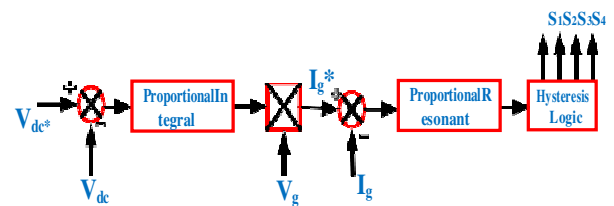


Figure 12. PR Controller for EV circuit configuration

Reference dc voltage and actual dc voltage are compared and the voltage error obtained is passed through a PI controller to generate the grid current reference for the current loop. Switching pulses for the IGBT switches of the single phase converter is generated by using hysteresis logic. Accordingly the frequency response characteristics shown in Fig. 13 are obtained for different values of ω_c from 0 to 25 rad/s. The proportional gain is taken as 1. It is observed that the bode plots converge to 20db/dec for any value of ω_c .

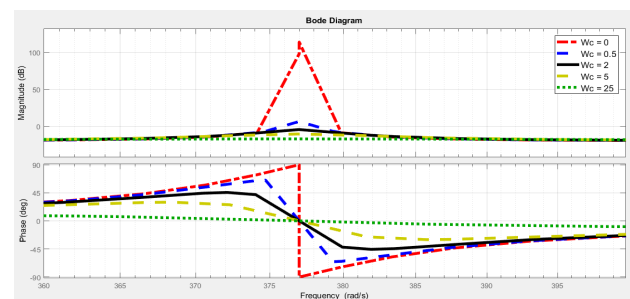


Figure 13. Frequency response characteristic for variation in ω_c and $k=1$

TABLE III. CIRCUIT CONFIGURATION PARAMETERS

Circuit Variables	Ratings
Grid voltage V_g	120 Vrms
Power frequency f_s	60 Hz
AC Filter inductor L_s	0.75 mH
AC Filter capacitor C_s	20 μ F
DC Capacitor C_{dc}	2 mF
Inductor L_o	41 μ H
Capacitor C_o	600 μ F
Battery capacity	100 AH
Hysteresis band h	± 0.5 V
PR Controller parameters K_p, T_i	100, 0.1 ms

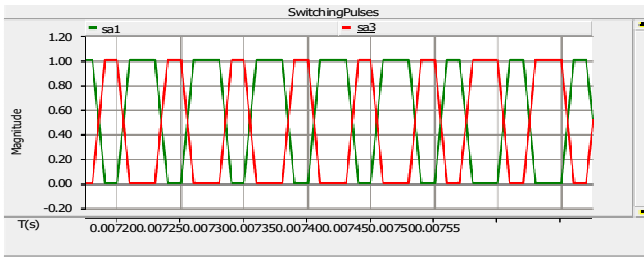


Figure 14. Switching pulses to the Bidirectional AC-DC Converter switches

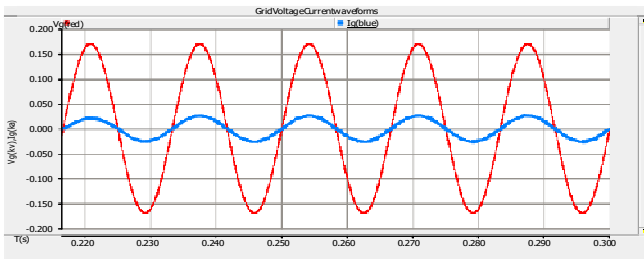


Figure 15. Grid Voltage and Current waveforms during charging

TABLE IV GRID VOLTAGE AND CURRENT HARMONIC COMPONENTS

Harmonic order	Individual Current THD%	Voltage Individual THD%
3	1.804	0.0220
5	1.604	0.0072
7	0.708	0.0203
9	0.192	0.0052
11	0.590	0.0078
13	1.235	0.0133

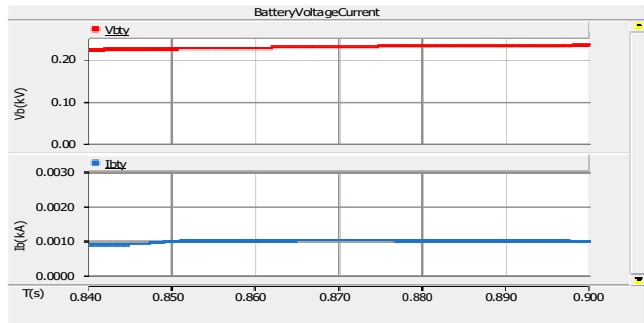


Figure 16. Battery charging Voltage and Current

The peak amplitude of the gain margin increases with lower values of ω_c . It also reveals that the infinite gain only occurs at resonant frequency. Therefore the PR controller is sensitive between controller resonant frequency and fundamental frequency of the converter. Hence the sensitivity can be reduced by taking a small value of ω_c . In this work 10 rad/s is taken. A trade off should be made by properly selecting the value of k and ω_c .

Fig. 14 shows the switching pulses applied to bidirectional AC-DC converter during the charging of the electric vehicle. Fig. 15 shows the grid current and voltage in charging mode of operation with PR controller. The input voltage and current is in phase with each other. Fig. 16 shows the battery current and voltage waveforms during charging, the voltage waveform has small increase and the current waveform is constant. Fig. 17 shows the battery SOC waveform during battery charging. The odd order harmonic component presenting grid voltage

and current during the charging is shown in Table IV. It is observed that 3rd and 5th order harmonic component is more compared to 7th, 9th, 11th and 13th, voltage and current THD is within the IEEE-519 standards.

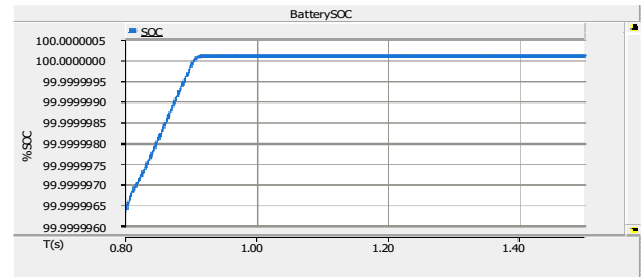


Figure 17. SOC during charging

V. ELECTRIC VEHICLE SUPPORT TO GRID

In this mode of operation bidirectional AC-DC converter acts as an inverter and controls output grid current. The battery supplies power to grid based on the requirement of the power grid and the convenience of the EV owner. The simulation results are presented in this section.

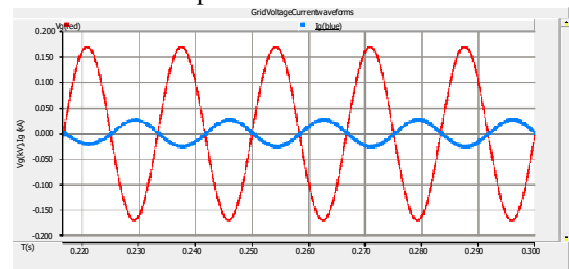


Figure 18. Grid Current and Voltage Current waveforms

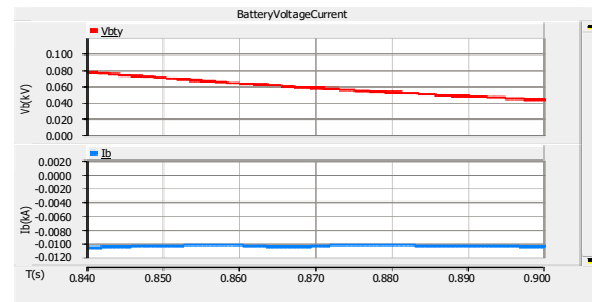


Figure 19. Battery discharging Voltage and Current

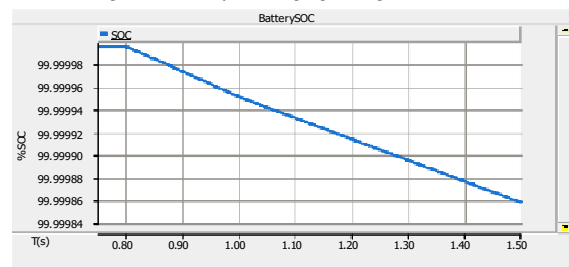


Figure 20. SOC during discharging

The grid voltage and current waveforms during discharging is shown Fig. 18, in charging the grid voltage and current is in phase but in discharging the grid current is out of phase to the grid voltage. It shows that power flows from EV battery to

the power grid. Fig. 19 shows the battery voltage and current waveforms during battery discharging, the voltage waveform is decreasing and current wave is constant. Fig. 20 shows the SOC of the battery during discharging.

VI. CONCLUSIONS

This paper presents an electric vehicle charging circuit with solar energy as a source. The PV array is tested under standard test conditions, the Current-Voltage and a Power-Voltage characteristic of the solar PV is obtained. Passive filter parameters design methodology is presented. The solar PV is designed to produce the output voltage of 200V which is stepped to 400 V using a boost converter. The output voltage is filtered and this filtered voltage is step down according to EV Battery charging requirements by using a buck converter. The PR controller used is efficient in charging the EV battery. SOC is observed to be efficient during charging and discharging modes. A corner frequency of 10 rad/s has been selected properly based on frequency response characteristic. The EV charging from grid and battery energy fed back to grid are illustrated with voltage and current in-phase and out of phase respectively. Grid current and voltage THD levels follow IEEE 519 standards. The SOC of the battery is obtained during battery charging and discharging operation. The controller is good in tracking the reference voltage during both charging and discharging with less steady state error.

Solar charging overcomes voltage problems and overloading in the distributed network due to more generating units and increased demand of power due to more number of EVs charging from the grid.

REFERENCES

- [1] Nian Liu, Oifang Chen, Xinvu Lu, Jie Liu and Jianhua Zhang, "A Charging Strategy for PV-Based Battery Switch Station Considering Service Availability and Self-Consumption of PV Energy," *IEEE Trans. Ind Electronics.*, vol.62, no.8, pp.4878-4889, Feb 2015.
- [2] K. Chaudhari, A. Ukil, K. N. Kumar, U. Manandhar and S. K. Kollimalla, "Hybrid Optimization for Economic Deployment of ESS in PV-Integrated EV Charging Stations," *IEEE Trans. Ind. Informatics*, vol. 14, no. 1, pp. 106-116, Jan 2018.
- [3] Bhim Singh, Anjeet Verma, A. Chandra and Kamal Al-Haddad, "Implementation of Solar PV-Battery and Diesel Generator Based Electric Vehicle Charging Station," in *IEEE International Conference on Power Electronics, Drives and Energy Systems (PEDES)*, 2018.
- [4] Hoang N. T. Nguyen, Cishen Zhang, and Jingxin Zhang, "Dynamic Demand Control of Electric Vehicle to Support Power Grid With High Penetration Level of Renewable Energy," *IEEE Trans. Transportation Electrification*, vol. 2, no. 1, pp. 66-75, Mar 2016.
- [5] Tan Ma and Osama A. Mohammed, "Optimal Charging of Plug-in Electric Vehicles for a Car-Park Infrastructure," *IEEE Trans. Industry Applications*, vol. 50, no. 4, pp. 2323-2330 July/Aug 2014.
- [6] G. Satish Kumar and Bikram Sah, "A Comparative study of different MPPT techniques using different dc-dc converters in a standalone PV system," in *IEEE TENCON Singapore*, November 2016.
- [7] V. Monteiro, J. G. Pinto and J. L. Afonso, "Operation modes for the electric vehicle in smart grids and smart homes: Present and proposed modes," *IEEE Trans. Veh. Technol.*, vol. 65, no.3, pp.1007-1020, Mar 2016.
- [8] M. C. Kisacikoglu, B. Ozpineci, and L. M. Tolbert, "EV/PHEV bidirectional charger assessment for V2G reactive power operation," *IEEE Trans. Power Electron.*, vol. 28, no. 12, pp. 5717-5727, Dec. 2013.
- [9] By Xiaosong Hu, Chagfu Zou, Caiping Zhang, And Yang Li, "Technological Developments in Batteries" *IEEE power & energy magazine*, pp. 20- 31, Sep/Oct 2017.
- [10] X.Zhou, S.Lukic, S.Bhattacharya, and A.Huang, "Design and control of grid-connected converter in Bi-directional battery charger for plugin hybrid electric vehicle application," in *Proc. IEEE Veh. Power and Propulsion Conf.*, pp. 1716-1721, Sep 2009.
- [11] D.N. Zmood, D.G. Holmes, "Stationary frame current regulation of PWM inverters with zero steady-state error," *IEEE Trans. Power Electron.*, vol. 18, no.3, pp. 814-822, May 2003.
- [12] A.V.J.S.Praneeth, Najath A Azeez, Lalit Patnaik, Sheldon S Williamson, "Proportional Resonant Controllers in On-board Battery Chargers for Electric Transportation," *IEEE International Conference on Industrial Electronics for Sustainable Energy Systems (IESES)*, pp.237-242, 2018.